Production of Hydrogen Peroxide in Groundwater at Rifle, Colorado

Xiu Yuan[*,†], Peter S. Nico[†], Xiang Huang[‡], Tongxu Liu[§], Craig Ulrich[†], Kenneth H. Williams[†], and James A. Davis[†]

[†] Earth and Environmental Sciences, Lawrence Berkeley National Laboratory, 1 Cyclotron Road, Berkeley, California 94720, United States

[‡] Institute of Water Sciences and College of Engineering, Peking University, 5 Yiheyuan Road, Haidian, Beijing 100871, China

[§] School of Civil and Environmental Engineering, University of New South Wales, Sydney, New South Wales 2052, Australia

DOI: 10.1021/acs.est.6b04803

Publication Date (Web): June 14, 2017

*X. Yuan. Tel.: +1 (510) 486-7684, Email: xiuyuan@lbl.gov.

Abstract

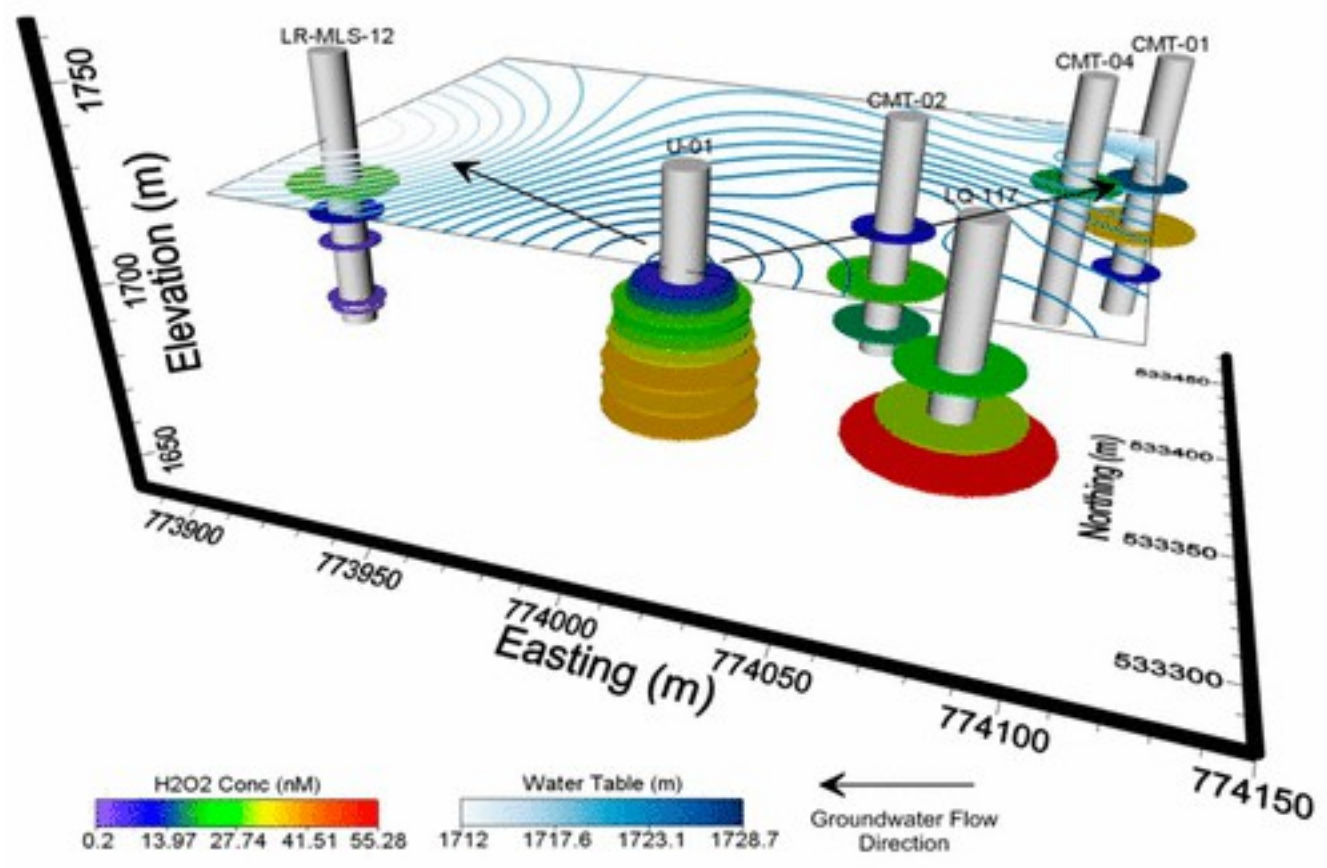

The commonly held assumption that photodependent processes dominate H_2O_2 production in natural waters has been recently questioned. Here, we present evidence for the unrecognized and light-independent generation of H_2O_2 in groundwater of an alluvial aquifer adjacent to the Colorado River

near Rifle, CO. In situ detection using a sensitive chemiluminescent method suggests H_2O_2 concentrations ranging from lower than the detection limit (<1 nM) to 54 nM along the vertical profiles obtained at various locations across the aquifer. Our results also suggest dark formation of H_2O_2 is more likely to occur in transitional redox environments where reduced elements (e.g., reduced metals and NOM) meet oxygen, such as oxic–anoxic interfaces. A simplified kinetic model involving interactions among iron, reduced NOM, and oxygen was able to reproduce roughly many, but not all, of the features in our detected H_2O_2 profiles, and therefore there are other minor biological and/or chemical controls on H_2O_2 steady-state concentrations in such aquifer. Because of its transient nature, the widespread presence of H_2O_2 in groundwater suggests the existence of a balance between H_2O_2 sources and sinks, which potentially involves a cascade of various biogeochemically important processes that could have significant impacts on metal/nutrient cycling in groundwater-dependent ecosystems, such as wetlands and springs. More importantly, our results demonstrate that reactive oxygen species are not only widespread in oceanic and atmospheric systems but also in the subsurface domain, possibly the least understood component of biogeochemical cycles.

1 Introduction

Reactive oxygen species (ROS), such as superoxide ($O_2^{\bullet-}$), hydrogen peroxide (H_2O_2), and hydroxyl radical ($HO^{\bullet}$), are intermediates generated during the sequential one-electron reduction of O_2 to H_2O. (1) These oxygen-containing reactive molecules, though generally present in natural environments at particularly low concentrations (picomolar to micromolar), are of considerable importance due to their transient nature and outstanding capability of oxidizing a wide range of molecules with relatively low selectivity.(2, 3) Extensive studies have shown that ROS are involved in various biogeochemical and ecologically significant processes,(4) such as the formation of manganese oxides,(5, 6) coral bleaching,(7) algal bloom-mediated massive fish kills,(8) and the establishment of microbial symbioses.(4, 9) In addition, recent increasing recognition of the important roles of ROS in carbon remineralization,(10, 11) metal bioavailability,(12) and contaminant transport urges a more comprehensive understanding of ROS generation and transformation in natural environments.

Because of the transient nature of ROS and the challenges associated with direct measurement of their production capacity in a given environment, field investigations of ROS have mainly focused on H_2O_2, simply because it has a longer half-life (ranging from hours to days in water) and is thus much

more stable than $O_2^{\cdot-}$ and $HO^{\cdot}$.(13) H_2O_2 is ubiquitous in natural waters and can act as an oxidizing or reducing agent to react with a large suite of biologically important and redox-sensitive trace elements, such as iron,(14-16) copper,(17-19) chromium,(20, 21) and arsenic.(22, 23) The dominant source of H_2O_2 in natural waters has long been attributed to photo-oxidation of chromophoric dissolved organic matter (CDOM) by molecular oxygen, with various studies addressing H_2O_2 patterns (from undetectable to greater than 1000 nM) in a wide range of surface waters, including oceans,(24-27) coastal and estuarine waters,(28, 29) lakes,(30-32) freshwater,(33-35) and geothermal waters.(36, 37) However, recent studies indicated that dark production of H_2O_2 in deep seawater, likely of biological origin, is potentially on par with its photochemical origins.(13, 38-40) For example, Wu et al.(13) reported persistent high H_2O_2 concentrations at water depths exceeding 80 m in Northern South China Sea Shelf-sea, where solar irradiance was virtually absent, and suggested various processes, such as dark biological production, trace metal mediated redox reactions, as well as physical mixing, could all contribute to such observed vertical distribution. Further, atmospheric H_2O_2, acting as a useful indicator of radical levels in the atmosphere to imply how the troposphere changes with time in response to natural and anthropogenic perturbations, has also received a great deal of attention in atmospheric oxidant studies.(41-45) Concentrations of H_2O_2 in atmospheric samples have been reported to be correlated with solar radiation, humidity, temperature, as well as concentrations of O_3, NO_x, and hydrocarbons.(41) More interestingly, H_2O_2 has also been detected in the atmosphere of Mars, with a typical concentration of 500–1200 nM, possibly generated by triboelectricity during dust storms or dust devils of the red planet.(46, 47)

Although some preliminary insights into the likely concentrations of H_2O_2 in natural waters (both surface and deep oceans) and atmospheric systems are now available, there is a severe dearth of information regarding H_2O_2 generation and patterns in the subsurface systems, a large but poorly understood domain in our global habitat. Unlike the surface environment, subsurface systems are generally O_2-deficient, which is presumably the reason that ROS production in such underground territory has been overlooked. However, the redox conditions of subsurface environments are often perturbed by O_2 from both natural and anthropogenic processes (e.g., groundwater fluctuations in response to rainfall, groundwater recharge by treated wastewaters, hyporheic exchange, riverbank filtration, soil flushing, farming and construction activities, as well as flood events), leading to alterations of local biogeochemical settings and strong interactions between $O_2$and reduced components. Although Tong et al.(10) reported significant ROS generation from a variety of typical redox-fluctuating subsurface environments, Page et al.(11) observed dark formation of $HO^{\cdot}$ by oxidation of reduced soil waters from the arctic tundra, with the highest formation rate predicted at

oxic–anoxic boundaries in arctic soil and surface waters. Another study by Zhang et al.(1) observed the occurrence of dark biological production of H_2O_2 along the depth profiles of several brackish and freshwater ponds. As a consequence, if dark production of H_2O_2 is prevalent in deep ocean, sediments, and fresh waters (either of biological or chemical origin), there is no reason to exclude H_2O_2 sources in shallow groundwater systems, especially in unconfined aquifers, where extensive interactions among oxygen, microorganisms, natural organic matter, and various trace elements take place. Here, we present evidence for the unrecognized and light-independent generation of H_2O_2 in the groundwater of an alluvial aquifer adjacent to the Colorado River near Rifle, CO. Our results suggest that detectable H_2O_2 concentrations are common, ranging from lower than the detection limit (<1 nM) to 54 nM along the vertical profiles in groundwater at several locations across the Rifle site. Recognition of ROS sources in groundwater systems not only helps us better understand their potential impact on metal/nutrient cycling on groundwater-dependent ecosystems, such as wetlands and springs, but also further advances our knowledge of the role played by H_2O_2 and associated intermediates (such as $O_2^{\cdot-}$ and $HO^{\cdot}$) in ecosystems as a whole.(29)

2 Materials and Methods

2.1 Reagents

Analytical grade chemicals were purchased from VWR International or Sigma-Aldrich (or as otherwise stated) and used without further refinement. Acridinium ester (AE, 10-methyl-9-(*p*-formylphenyl)acridinium carboxylate trifluoromethanesulfonate) was purchased from Cayman Chemical (Michigan, USA). AE reagent of 5.0 μM at pH 3.0 was prepared each sampling day by dilution of a refrigerated AE stock solution (250 μM, pH 3.0) by adding 1.0 mM phosphate buffer (pH 3.0). H_2O_2 (30%, ultrahigh purity) was purchased from BDH Chemicals and calibrated spectrophotometrically using a UV–vis spectrophotometer. 0.1 M carbonate buffer of pH 11.3 was prepared weekly, and other stock solutions were refrigerated at 4 °C in the dark.

2.2 Field Information and Experimental Measurement

Field Site and Groundwater Sampling

Groundwater samples were collected between May 21 and June 6, 2015 at the U.S. Department of Energy (DOE) Rifle, CO field site. The field site is located on a floodplain adjacent to the Colorado River and was a former uranium and vanadium mill operated between 1924 and 1958 (see Figure S1 for a high resolution site map and Yabusaki et al. (2007)(48) and Janot et al. (2016)(49) for more

information). Currently, this site supports research activities associated with Lawrence Berkeley National Laboratory.

H_2O_2 detection was performed by sampling groundwater through 11 wells, including a series of 3-port continuous multichannel tubing (CMT) wells installed along a transect aligned with the groundwater flow direction of the Rifle floodplain in 2014 (CMT01–CMT05, see Figure S2 for detailed location map and Figure S3 for borehole information on Well CMT01 as an example). Before sampling in each well, at least 24–30 L of water was slowly pumped out from the borehole, which is more than the total volume that could be held in each channel of the well, indicating the sampled water was freshly infiltrated from the nearby aquifer rather than the water initially present in the well. Sample water was peristaltically pumped through opaque flexible tubing into an amber high density polyethylene (HDPE) bottle with no head space and was analyzed within 4–6 min after collection. Filtration of the groundwater by 0.22 μm filters made no difference on the final concentration of H_2O_2; therefore, no filtration was done to minimize the sampling time.

H_2O_2 Analysis

In situ H_2O_2 concentrations were determined by the chemiluminescing reaction between acridinium ester (AE, 10-methyl-9-(*p*-formylphenyl)acridinium carboxylate trifluoromethanesulfonate) and the conjugate base of H_2O_2 (HO_2^-, pK_a = 11.6).(50, 51) The emitted luminescence at 470 nm was detected by flow injection analysis using a FeLume system (Waterville Analytical, Waterville, ME). To avoid any possible interference caused by additional interactions between ferrous iron and O_2 under alkaline conditions,(51) 2.0 mM Ferrozine solution (3-(2-pyridyl)-5,6-diphenyl-1,2,4-triazine-4′,4″-disulfonic acid sodium salt, Sigma) was added to bind all the ferrous species before the sample entered the flow cell located at the photo multiplier tube interface, where it mixed with a carbonate (pH 11.3) buffer to initiate the chemiluminescence-generating reaction. An acid-wash loop was also integrated to rinse off any possible precipitates formed by the groundwater at alkaline conditions. After each sample measurement, 0.01 M HCl flowed through the system for at least 3 min and followed by another 2–3 min of distilled deionized (DDI) water. Because of the ubiquitousness of H_2O_2 in most of the laboratory waters, analytical blanks were obtained by adding 3.0 mg L^{-1} catalase (the enzyme that decomposes H_2O_2 to water and O_2) to the DDI water used for preparation of reagents and buffer solutions at least 30 min ahead.(50) Catalase remaining in the reagent and buffer will inevitably react with some of the H_2O_2 in the sample. However, loss of sample H_2O_2 is insignificant because the half-life of H_2O_2 in 3.0 mg L^{-1} catalase is 15 min and the flow injection analysis time is less than 30 s.(50) The detection limit of H_2O_2 using analytical set up in this study is 1.0 nM determined from the calibration curves and the uncertainty in the blank.

Other Element Analysis

Dissolved oxygen (DO) concentrations were measured on site by DO CHEMets Visual Kits (CHEMetrics, Inc.), with Rhodazine D method(52) for DO < 1 ppm (Kit No.: K-7501) and Indigo Carmine method(53) for DO of 1–12 ppm (Kit No.: K-7512). Samples for elemental analysis and total organic carbon (TOC) measurement were collected and acidified to pH 3 with HCl (high purity, 30% w/v; Sigma) and kept cool or refrigerated until shipped to the laboratory in Berkeley, CA. TOC concentrations were measured using a Shimadzu TOC-V_{CSH} analyzer with an ASI-V autosampler (Shimadzu). Total element concentrations were determined by inductively coupled plasma mass spectrometry (ICP-MS, PerkinElmer SCIEX ICP-Mass Spectrometer ELAN DRC II).

Kinetic Modeling

The kinetic model was fitted to the experimental data over a range of experimental conditions using the program Kintek Explorer.(54)

3 Results and Discussion

3.1 Background H_2O_2 Profiles in Rifle Aquifer

The most finely resolved spatial profile of H_2O_2 (Figure 1) was obtained in Well U-01 (located in Experimental Plot A, see Figure S1 for well location map), showing a vertical concentration range of 7–38 nM. The occurrence of H_2O_2 is remarkable, not only because no H_2O_2 generation in groundwater has been previously discovered, but also the permanent absence of light, low abundance of DO, and the widespread reactive sediments in the subsurface system that would decrease the ambient concentrations of ROS. More interestingly, H_2O_2 concentrations observed in Well U-01 increased with water depth, with increasing concentrations in the upper half of the profile and almost constant and high H_2O_2 levels at lower depths. This also departs from our traditional expectation where photodependent processes are the dominant cause of H_2O_2generation. In other words, the typical profiles of H_2O_2 in surface waters have been widely reported to exhibit apparent diel cycles and decrease monotonically with water depth.(24-27, 33)However, exceptions to this trend have also been observed in various studies,(1, 13, 38, 55)implying that besides photoproduction, other factors related to H_2O_2 formation and/or decomposition may be important under certain conditions.

Figure 1. Depth profiles of H_2O_2, total iron, DO, and TOC concentrations in Well U-01. Samples were collected on May 24, 2015. Water table was 2.55 m below the ground surface. Error bars (some of which are too small to be visible) are the standard errors from triplicate measurements.

To discover correlations between H_2O_2 profiles and other potential critical elements, groundwater samples of Well U-01 were also characterized with respect to dissolved oxygen (DO), total iron concentration, and organic carbon content (TOC) (Figure 1). Information about other auxiliary parameters and elements is presented in Table S1. As shown in Figure 1, it is noteworthy that more than 70 μM DO was observed throughout the depth of this well, with the maximum concentration of 143 μM occurring 0.91 m below the water table (3.47 m below the ground), and a lower concentration of 72 μM present at the bottom. Such levels of DO in groundwater were not unexpected because oxygen can be transported faster than it is consumed in permeable sediments, and anoxic conditions are more difficult to achieve near the water table.(49) At the same time, DO in the Rifle aquifer is also tied to seasonal variations in groundwater elevation,(56)with a rising water table bringing more oxygen into the system and stronger vertical mixing between water layers. The dissolved organic carbon concentration was generally constant (~290 μM) throughout the vertical profile, except one higher concentration of 340 μM right below the water table. In surface waters, although the variations in the concentrations of H_2O_2 and TOC have been found to exhibit close correlations (consistent with the fact that CDOM is the primary control on photochemical production of H_2O_2),(13) a nonuniform relationship between CDOM or dissolved organic matter fluorescence and the photochemical production rate of H_2O_2 has also been observed in several studies.(13, 26, 28) On the other hand, formation of $HO^{\cdot}$ (through the intermediacy of H_2O_2) during oxidation of reduced organic matter under dark conditions represents a previously unknown source of $HO^{\cdot}$ formation at oxic/anoxic boundaries and may affect the biogeochemical and pollutant redox dynamics at these interfaces.(57)

In the subsurface, Fe(II) mainly exists in the form of complexes in pore water and minerals in sediments and has been reported to be involved in the generation and/or decomposition of H_2O_2.(10, 57) The vertical profile of dissolved iron in groundwater at Well U-01 (Figure 1) covered a narrow range of 260–540 μM. Though not characterized in this study, essentially all of this dissolved iron was present as Fe(II).(58) A recent study that characterized the heterogeneity of organic-rich sediment in the Rifle aquifer observed abundant mackinawite (FeS) in the sediments from the capillary fringe above naturally reduced zones (NRZs), indicating that certain reducing conditions are present in the oxic portion of the aquifer, probably maintained in the interior of aggregates within organic-rich sediments.(49) The heterogeneously dispersed NRZs in the Rifle aquifer are

characterized by high concentrations of organic carbon, reduced mineral phases, and reduced forms of metals, including Fe(II), uranium(IV), and vanadium(IV). These reduced metals in the NRZs are seasonally exposed to oxygen and contribute to formation of $O_2^{\cdot-}$, the widely accepted immediate precursor of H_2O_2 (though an alternative mechanism might occur when biologically mediated processes predominate(40, 59, 60)). On the other hand, Fenton and Fenton-like reactions induced by reduced trace metals have also been indicated to promote the decomposition of H_2O_2 and generation of more reactive oxidants, including $HO^{\cdot}$ and high valent Fe species.(61, 62) For instance, generation of $HO^{\cdot}$ from oxidation of ligand-complexed Fe(II) by O_2 has been confirmed in laboratory studies and utilized for degradation of organic pollutants in wastewaters.(62) Therefore, in a system with the presence of oxygen, reduced metals and natural organic matter (NOM), H_2O_2 can be generated from oxygenation of reduced elements and metal-mediated oxidation of NOM,(14, 18, 63) whereas reduced metals and NOM (dissolved and in sediments), at the same time, could also act as sinks by further reacting with H_2O_2.(23) Thus, the relationships between H_2O_2 concentrations and iron/organic carbon content could be rather complex, largely depending on the biogeochemical settings of the specific environmental system. Various other factors, including pH, temperature, biologically mediated generation and decomposition, variability and redox properties of NOM, and the presence of various scavengers, could all influence the temporal and spatial patterns of H_2O_2 in the groundwater. As a consequence, no simple correlations between H_2O_2 and DO, total Fe, or TOC profiles were evident in this study, and the exact mechanisms causing the observed vertical distributions of H_2O_2 in Rifle groundwater cannot be stated with confidence at this stage. Nevertheless, one explanation could be the effect of dark biological production associated with different bacterial activity with distance from the water table, and none of the examined elements (DO, total Fe, or TOC), was the rate-determining factor.

Wu et al.(13) indicated in their recent study of tropical shelf waters that concentrations of H_2O_2were generally elevated at places where the activity of internal waves and mixing was extensive, but in this study, no H_2O_2 was observed in another location (Well 310, Figure S2), which is ~30 m closer (compared to Well U-01) to the Colorado River bank. Thus, mixing of water from the river should not be a significant contributor, at least not in the Rifle groundwater. This is further confirmed by another vertical profile of [H_2O_2] that was obtained at the location of Well LR12 (Figure 2), a multilevel sampling (MLS) well (detailed diagram of the MLS construction was shown in a previous study(58)) located in Experimental Plot B (Figure S1). H_2O_2 concentrations ranged from 28 nM near the water table to lower than the detection limit (<1 nM) at the bottom of this borehole. Similar to H_2O_2 profile, concentrations of other relevant solutes (DO, total Fe, and TOC) decreased along the water depth,

with the only exception occurring at a depth of 4.3 m below the water table. Unlike the conditions at Well U-01, significant O_2-deficiency (DO < 2.5 μM) was found throughout the depth of this well, which might exert a limiting factor for in situ H_2O_2 formation. However, Borda et al.(64) and Zhang et al. (23) reported production of H_2O_2 and $HO^{\cdot}$ from the oxidation of H_2O at sulfur-deficient sites on pyrite surface under anoxic conditions, demonstrating that O_2 is not necessarily a prerequisite for ROS generation under some circumstance. The sharp decrease of H_2O_2 in the upper-half of the vertical profile at Well LR12 may be correlated to the notable decrease of total iron and TOC concentrations at the same elevation, while the distinguishable rebound at 4.3 m below the water table happened simultaneously with locally higher level of DO and total iron.

Figure 2. Depth profiles of H_2O_2, total iron, DO, and TOC concentrations in Well LR12. Samples were acquired on June 04, 2015. Water table was 3.20 m below the ground surface. Error bars (some of which are too small to be visible) are the standard errors from triplicate measurements.

Various concentrations of H_2O_2 (range of 10–54 nM) were also detected in a few other locations of this aquifer (3-port CMT wells, detailed elevations presented in Table S2), as collectively shown in Figure 3. Interestingly, the highest H_2O_2 concentrations at all these wells happened coincidentally in groundwater that was located 2.0–3.0 m below the water table. Another recent study on dark biological production of ROS in brackish and freshwater systems(1) reported that ROS ($O_2^{\cdot-}$ and H_2O_2) generation rates peaked at 2.0–4.0 m below the water surface and H_2O_2 profiles did not show apparent dependence on the water depth in the aphotic zone. To be more specific, in freshwater system, photosynthetically active radiation (PAR) declined to 3.1% and 0.9% of the surface level at 3.5 and 4.5 m below the water surface, whereas H_2O_2 concentrations were 65.6% and 87.2% of that in surface water,(1) indicating that light-intensity might not be the limiting factor for H_2O_2 formation at these depths. Such atypical H_2O_2 profiles in their study were mainly attributed to biological production and possible vertical mixing throughout the shallow waters.(1) At the same time, Tong et al.(10) also found that during oxygenation of various sediments, the generation rate of $HO^{\cdot}$ increased significantly with the sample depth of the sediments, suggesting that the more reduced the sediments, the more $HO^{\cdot}$ will be produced after exposure to oxygen. During our sampling time (May to June 2015), the water table at the Rifle site was increasing quickly (Figure S4), a situation typical during later spring/early summer in the Colorado river basin when the river stage is rising as a result of snowmelt. Such seasonal change in water table inevitably brings more oxygen into the

groundwater, and thus alters local redox conditions and biogeochemical settings in the aquifer. For example, introduction of O_2 into the region below the water table creates oxic–anoxic boundaries, where anoxic waters mix with oxic flows and thus initiates cascade redox reactions. Of particular interest here is the generation of large amounts of ROS under such fluctuating redox conditions that has been recently identified in several studies.(1, 10, 11, 16, 65) The observed H_2O_2 spike occurring at 2.0–3.0 m below the water table in various locations of the Rifle aquifer (Figure 3) could be caused by intensive ROS generation at oxic–anoxic interfaces resulting from seasonal variations in the groundwater table. In fact, not only natural processes, such as groundwater fluctuations and recharge, hyporheic exchange and episodic, high intensity events (like storms and floods), but also anthropogenic activities, including soil flushing, groundwater replenishment, farming and construction activities, could all result in the formation of oxic-anoxic mixing zones where oxygen concentrations vary intermittently and considerable amounts of ROS are generated. A recent estimate(16) based on radium isotope inventories suggested that approximately 6.0×10^{10} kg of water exchanged between oxic and anoxic conditions per day for the entire South Carolina coastline, which implied a potential abiotic ROS flux of up to 1.5×10^{7} moles day^{-1}, comparable in magnitude to photochemical sources of ROS in surface waters (including coastal and seawaters).(66, 67) More importantly, such sustained ROS generation may also contribute to global carbon cycling by breaking down otherwise recalcitrant organic compounds (such as bisphenol A, and polycyclic aromatic hydrocarbons)(57, 68) into better microbial energy sources, an alternative but important pathway for microbial alteration and consumption of natural and anthropogenic organic carbon.

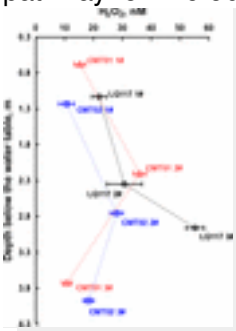

Figure 3. H_2O_2 concentrations at various depths of different CMT wells in the Rifle site. Water table was below the ground surface: CMT01, 3.22 m; CMT02, 1.76 m; LQ117, 1.71 m. Error bars (some of which are too small to be visible) are the standard errors from triplicate measurements.

Overall, detectable H_2O_2 was found at six of the eleven locations that we measured at the Rifle aquifer, besides the aforementioned five wells that had H_2O_2 along the full depth of the well, 19.7 nM H_2O_2 was found at 0.28 m below the water table of Well CMT04, but no H_2O_2 was observed below

this depth, possibly because of the severe O_2 deficiency at the bottom of the well (Table S1). It is noteworthy that all of the five wells where no H_2O_2 was detected uniformly had extremely low concentrations of DO (generally DO < 0.1 mg/L), whereas most of the locations where $H_2O_2$was detected exhibited higher DO concentrations, except Well LR12, of which detectable H_2O_2(up to 28 nM) was found in groundwater with remarkably low DO (Figure 2). At the same time, for the deep elevation of CMT04 and all depths of CMT05, constant high concentrations of iron and manganese (Table S1) were observed in the absence of H_2O_2, indicating that under reducing conditions such metal species may act as H_2O_2 consumers, rather than contributing to H_2O_2formation by reducing O_2. (57)

3.2 Dark Formation of H_2O_2 in O_2 Injection Experiments

In addition to background H_2O_2 detection in the aquifer, O_2 injection field experiments were also conducted to investigate the oxidation of naturally reduced uranium in Rifle aquifer sediments and its potential significance to uranium plume persistence.(69) Briefly, groundwater (~772 L) from the naturally reduced zones in wells of JB04 and JB02 (Figure S2) was pumped into an opaque and gas-impermeable bag and mixed with a conservative tracer (Br^-). A gas phase composed of 97% O_2 and 3% CO_2 was continuously bubbled through the groundwater in the bag for 2.8 h. Then the groundwater with a high concentration of DO (0.66 mM) was pumped back into the subsurface in Well JB04. First of all, no background H_2O_2 was detected in groundwater sampled from wells JB04 and JB02 before the experiment. However, after bubbling O_2 into the bag, H_2O_2concentration of the groundwater in the bag reached 252 nM (Figure S5), demonstrating generation of ROS when O_2 is supplied to anoxic water. It is noteworthy that even though more than 250 nM H_2O_2 (in ~772 L water) was injected into Well JB04, immediate sampling at Well JB04 after the injection (total injection time ~ 2.9 h) showed no residual H_2O_2, indicating the existence of significant sinks in this location, and that all of the injected H_2O_2 was consumed quickly in the local groundwater. However, 40–60 h after the injection, relatively high concentrations of H_2O_2 were detected at adjacent down-gradient wells (maximum concentrations of 97 and 213 nM in JB02 and JB05, respectively, Figure S6), as shown in Figure 4 (see Figure S2for location map of these two adjacent wells). It is reasonable to speculate that the observed concentrations of H_2O_2 in these downgradient wells could have been originated from the H_2O_2initially generated in the injection bag. That is, the 252 nM H_2O_2 generated in the 772 L of injection water was not completely consumed at the injection spot of JB04, instead it moved downstream to wells of JB02 and JB05 after 40–60 h of transport. However, if we assume that the unconsumed H_2O_2 (if there was any) from JB04 would transport downstream in a pattern similar to that of Br^-, it is worth noting that the normalized concentrations of H_2O_2 (the concentration divided by the injected H_2O_2 concentration) at these wells had a very different breakthrough pattern than Br^-

(Figure 4), especially for JB05, where the value of C/C_0 for H_2O_2 was much higher than that for Br^-. These results illustrate that the detected H_2O_2 patterns at wells of JB02 and JB05 could not be totally attributed to H_2O_2 from the injected water and H_2O_2 was not conservative during transport downgradient due to the presence of various sources and sinks. Moreover, the estimations in Figure 4 were based on the assumption that there was no H_2O_2 consumption during the transport, which almost certainly was not the case, because no H_2O_2 was detected in JB04 immediately after the injection, indicating that consumption along the flow path was indeed significant. As a consequence, ~200 nM H_2O_2 detected throughout the three channels of JB05 had to be actively produced along the flow path, or perhaps in the vicinity of the sampling location in order to balance such rapid decomposition. Even though H_2O_2 has a relatively long lifetime (hours to days) in the absence of reactive solutes,(13) it is more likely that the abundant reduced species in the local environment around the wells consume H_2O_2 rapidly and prevent it from traveling a great distance. Although the reason that more H_2O_2 was produced in JB05 than JB02 (the closer well to JB04) could not be determined with certainty, dark biological production coupled with spatially variable bacterial activity in the aquifer could potentially be one of the causes, because soils are the most heterogeneous parts of the biosphere, with an extremely high variability of properties and processes within nano- to macroscales.(70) It has been reported that physicochemical and redox conditions of the Rifle aquifer differ vertically on a cm scale and laterally on a scale of less than 2 m. (49) Accordingly, highly diverse and dynamic microbiological zonations are more likely to exist in such a heterogeneous aquifer.(49) Besides, Murphy et al.(16)recently reported that when anoxic groundwater moved through oxidized, Fe(III) rich sediments, the presence of sulfide could rapidly reduce Fe(III) to Fe(II) and thus trigger a cascade of redox reactions between oxygen and iron species (with Fe(II) acting as an electron shuttle between reduced S species and O_2), leading to significant ROS generation. These observations point to a dynamic redox cycling of iron, sulfide, and H_2O_2 upon introducing oxygen into the aquifer, either by experimental perturbations, such as the oxygen injection of this study, or through more widespread natural processes like seasonal variations of groundwater elevation.

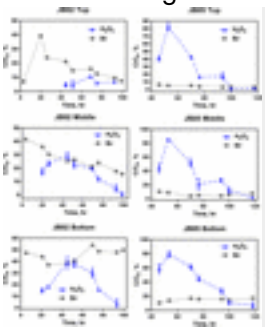

Figure 4. H_2O_2 and Br^- concentrations in downstream wells (JB02 and JB05) after oxygenated groundwater was injected in an adjacent upstream well JB04 (injection at JB04 started at t = 0). 1.10 mM NaBr was added to the injection water as a conservative tracer. C_0 of [Br^-] = 1.10 mM and C_0 of [H_2O_2] = 252 nM (the last concentration detected in the injection tank, as shown in Figure S5). Error bars (some of which are too small to be visible) are the standard errors from triplicate measurements. Detailed elevation information on the "top, middle, and bottom" baffles is provided in Table S2.

3.3 Mechanistic Insights of H_2O_2 Generation and Decomposition in Subsurface Systems

As previously stated, there are multiple pathways contributing to H_2O_2 generation and decomposition in the subsurface system, including dark biological production and consumption, redox cycling of metal species (either dissolved or in sediments) driven by fluctuating dissolved oxygen levels, and metal-mediated oxidation of reduced organic matter. First of all, there is increasing evidence indicating that many groups of microorganisms, including fungi, various species of phytoplankton and microalgae, symbionts in corals, and heterotrophic bacteria, are capable of extracellular ROS production.(1, 13, 71) One recent study by Zhang et al.(1) attributed their observed dark profiles of H_2O_2 in several brackish and freshwater ponds to biological sources since the addition of formaldehyde, which is capable of rapidly killing microorganisms within the water, significantly inhibited the dark particle-associated production of H_2O_2 in all of their samples. Although the biological groups in the subsurface domain that are actively involved in H_2O_2 production are not known, they may be one of the important contributors to the observed H_2O_2 patterns in the Rifle groundwater.

Despite the existence of a small portion of ROS production that was not inhibited by formaldehyde in the study by Zhang et al.,(1) Tong et al.(10) reported that sterilization of sediments led to only a negligible difference in $HO^{\cdot}$ accumulation under oxic conditions, while Dixon et al.(72) observed sterilization could eliminate the majority but not all of the H_2O_2 decay in dark incubations of soil suspensions, both pointing out that in addition to the biological origin, abiotic reactions, more or less, contribute to the formation and consumption of H_2O_2. Of particular interest here is the recently identified ROS production/decomposition resulted from oxygenation of various reduced elements that are widely presented in the subsurface domain. For instance, Page et al.(11)suggested cascade occurrence of dark ROS formation in environments where reduced NOM and Fe(II) produced by anaerobic microbial respiration are exposed to O_2, such as at oxic–anoxic interfaces. Therefore, under fluctuating redox conditions, H_2O_2 can be generated via interactions between oxygen and (a) reduced elements such as Fe(II) present either in pore water, adsorbed to sediment surfaces or within the structure of subsurface minerals (such as pyrite and mackinawite); or (b) reduced organic

moieties (such as hydroquinones) present in dissolved or soil organic matter, especially in the presence of transition metal species (such as iron and copper).(14, 18, 19, 73) Although the oxidation of dissolved Fe(II) by oxygen has long been reported to result in production of ROS,(74-76) oxygenation of Fe(II) species that are adsorbed to clays or oxides has also been recognized to occur at a substantially greater rate than the homogeneous oxygenation of Fe(II),(77) both accompanied by the formation of $O_2^{\cdot-}$ as a byproduct and subsequent formation of H_2O_2 by its disproportionation. With respect to Fe(II) minerals, recently Tong et al.(10) reported an abundant generation of $HO^{\cdot}$ (with H_2O_2 acting as the intermediate) on oxygenation of 33 subsurface sediments sampled from a variety of typical redox-fluctuating subsurface environments and found that Fe(II)-containing minerals, particularly phyllosilicates, are the predominant contributor to $HO^{\cdot}$ formation. Significant amounts of H_2O_2 are also formed during the oxygenation of pyrite(23, 78) and mackinawite(79, 80) over a wide range of conditions. Meanwhile, it is clear that these various forms of Fe(II) species not only contribute to H_2O_2formation but also are involved in subsequent transformation of H_2O_2 to $HO^{\cdot}$ through Fenton reactions, thus enhancing microbial degradation of natural organic materials by generating smaller soluble organic compounds from macromolecules and contributing to carbon and metal cycling in subsurface systems.

Previous studies on interactions between NOM and catalytic metal species under dark conditions demonstrate another pathway for ROS generation in the subsurface regime and provide a framework for modeling the generation of H_2O_2 as an intermediate during such redox processes.(14, 18, 19, 63, 73) Because the electron donating capacity (EDC) of NOM has been widely attributed to the presence of hydroquinone moieties within NOM that could be subsequently oxidized to semiquinone and quinone species, here we employed a recently reported kinetic model on iron-mediated oxidation of methoxyhydroquinone (MH_2Q) under dark conditions(14) as a simplified scenario to evaluate the impact of metal–NOM interactions on H_2O_2 formation in Rifle groundwater. Detailed model assumptions are presented in section SI4, and the full list of model reactions and rate constants(14) is shown in Table S3. Together with inputting the detected concentrations of DO and dissolved iron into the model, the predicted vertical distributions of H_2O_2in groundwater at Well U-01 and LR12 are shown in Figure 5. In general, modeled dark production of H_2O_2 from metal–NOM interactions was well predicted, or at least within a reasonable range to the measured vertical distributions of H_2O_2 at these locations. The “sink” role played by the exceptionally high concentration of iron right below the water table of LR12 might have been overestimated as a consequence of the model assumptions. To be more specific, the total iron concentrations detected at different well elevations were input to the model as reduced Fe(II), but these reduced species are likely to be

bound in various minerals or complexed by various organic ligands, thus possibly limiting their reactivity with H_2O_2. As a consequence, the actual “sink” role from reaction 10 (the Fenton reaction, Table S3) might be less important than predicted in the model, which may explain the larger mismatch between the model and the measured H_2O_2concentration at such depth. Meanwhile, it is also important to point out that in the model, it is assumed that all of the electrons donated by the reduced organic matter were transferred to Fe(III), whereas in the real environment, there must be various electron acceptors in the vicinity that act as efficient competitors with Fe(III) for those electrons, indicating that [H_2O_2] from the model output might be overestimated, such as in the model predictions for Well U-01. On the other hand, if the Fenton reaction (reaction 10, Table S3) was removed from the model, the output steady state concentrations of H_2O_2 under conditions for Well U-01 were around 1–2 μM, merely resulting from redox interactions among iron, hydroquinone, and oxygen. This again confirms the importance of metal–NOM interactions on ROS generation, as well as the “sink” effect resulting from the Fenton reaction in transforming H_2O_2 to $HO^{\cdot}$ in the system. For instance, it has been reported that a production rate of $HO^{\cdot}$ of 2–9 μmol L^{-1} d^{-1} from the Fenton reaction with a dissolved organic carbon concentration of 10 mg L^{-1} will be approached as long as enough Fe(II) is present to react with the formed H_2O_2,(81) suggesting that $HO^{\cdot}$ production from the Fenton’s reaction has the potential to cause significant effects on NOM transformation. In addition, a previous study in the Mediterranean and Baltic Seas(82) showed that both H_2O_2 production and decay rates in polluted water were higher than that at clean stations, indicating a more dynamic and influential role of H_2O_2 in pollutant transformation.

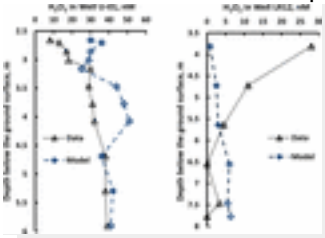

Figure 5. Detected and model predicted H_2O_2 concentrations along the depth profiles of Well U-01 and LR12. This is shown as one possible pathway contributing to dark H_2O_2 generation: the simplified interactions between metal and reduced organic matter. Modeled reactions and rate constants are shown in Table S3 and reported in Yuan et al. (2016).(14)

These observations have significant implications for micropollutant fate and carbon cycling and suggest a possible abiotic link between microbial metabolism and carbon oxidation. Recent research on global terrestrial ecosystem soil and vegetation components has suggested that soil organic matter contains more than three times as much carbon as either the atmosphere or terrestrial

vegetation,(83) and thus sustained ROS generation in the subsurface may represent an important pathway for global carbon cycling. Nevertheless, this model only represents one of the multiple pathways leading to H_2O_2 generation/decay and undoubtedly there are other sources and sinks of H_2O_2 in groundwater systems. Elucidating the importance of each pathway to the overall H_2O_2 patterns in the groundwater is beyond the scope of this study, but further studies are urged to reach a more comprehensive understanding of ROS generation and transformation in subsurface systems.

3.4 Implication of Findings

This study represents the first field measurement of light-independent H_2O_2 production in groundwater. Collectively, our results demonstrate that H_2O_2 profiles in groundwater at the Rifle site are highly spatially variable, largely depending on the features of the surrounding aquifer. There are many possible pathways shaping those H_2O_2 patterns, including dark biological production and consumption, metal-mediated oxidation of NOM, and cycling of metal species driven by fluctuating redox conditions. These results point to a need to understand better H_2O_2generation and cycling in the aphotic subsurface regime because of its potential importance to metal/nutrient cycling and contaminant mobilization in groundwater-dependent ecosystems.

This study also demonstrated that fluctuating redox conditions created at oxic/anoxic interfaces are likely to be “hot spots” for ROS generation: narrow boundaries in the aquifer with much faster process rates and much more intensive interactions compared to an average condition. Oxic/anoxic boundaries are ubiquitous in many natural environments, such as soils, sediments, and wetlands. Additionally, water tables in soils may fluctuate on the time scale of hours to days, leading to a relatively rapid succession of oxidizing and reducing conditions and hence repeated formation of H_2O_2 and other ROS species. Such highly reactive oxidants generated under dark conditions, similar to their photochemically produced counterparts, will inevitably promote carbon remineralization by decreasing the persistence of recalcitrant organic compounds and making them more susceptible to bacterial utilization or less resistant to chemical decomposition. Meanwhile, the sustained ROS formation at the oxic/anoxic boundaries may play a role in controlling the redox speciation of various trace metals and thus alter their bioavailability or toxicity in the subsurface environment, which may in turn affect the functioning of the ecosystem as a whole.

-

Supporting Information

The Supporting Information is available free of charge on the ACS Publications website at DOI: 10.1021/acs.est.6b04803.

- Additional detailed information on well locations at the Rifle site, measured auxiliary parameters of water samples, extra experimental data, and modeling development (PDF)

- **PDF**
  - es6b04803_si_001.pdf (1.31 MB)

Production of Hydrogen Peroxide in Groundwater at Rifle, Colorado

Supporting Information for the manuscript entitled
1
2
Production of Hydrogen Peroxide
in Groundwater at Rifle, Colorado
3
Xiu Yuan,
*
,
†
Peter S. Nico,
†
Xiang Huang,
‡
Tongxu Liu
,
§
Craig Ulrich
,
†
Kenneth H. Williams,
†
4
James A. Davis
†
5
†
Earth
and Environmental
Sciences, Lawrence Berkeley National Laboratory, 1 Cyclotron Road,
6
Berkeley, CA 94720, United States
7
‡
Institute of Water Science and
College of Engineering, Peking
University, 5 Yiheyuan Rd,
8
Haidian, Beijing 100871, China
9
§
School of Civil and Environmental
Engineering, University of New South Wales, Sydney, NSW
10

2052
,
Australia
11
12
13
Re
-
s
ubmitted
14
Environme
ntal Science & Technology
15
June
, 2017
16
17
18
* Corresponding author. Tel.: +1 (510) 486
-
7684,
19
Email:
xiuyuan@lbl.gov
20
21
Number of pages:
1
3
22
Number of figures:
6
23
Number of tables: 3
24
S
2
SI
1
.
Well locations and borehole information
of the Rifle Site
25
26
Fig.S1
.
Rifle integrated field researc
h challenge site (IFRC) base map
.
The image was acquired on behalf of the U.S. DOE for use in
27
the public domain in association with Berkeley Lab's research activities at the Rifle,
Colorado (USA) field site.
28

ShareDownload

The authors declare no competing financial interest.

Acknowledgment

The work reported here is supported as part of the Sustainable Systems (SS) Scientific Focus Area (SFA) program at LBNL, funded by the U.S. Department of Energy, Office of Science,Office of Biological and Environmental Research, Subsurface Biogeochemical Research Program, under Award Number DE-AC02-05CH11231. James A. Davis was supported by the Office of Legacy Management of the U.S. Department of Energy under Contract No. DE-AC02-05CH11231. The authors thank Richard Bush for his advice on specific work scope to address at the Old Rifle site, and gratefully acknowledge Chad Hobson (LBNL) and Noah Jemison from University of Illinois at Urbana–Champaign for their kind sampling assistance at the Rifle site.

Reference QuickView

References

This article references 83 other publications.

1. 1.

Zhang, T.; Hansel, C. M.; Voelker, B. M.; Lamborg, C. H. Extensive dark biological production of reactive oxygen species in brackish and freshwater ponds *Environ. Sci. Technol.* **2016**, 50 (6) 2983– 2993 DOI: 10.1021/acs.est.5b03906

[ACS Full Text], [CAS]

2. 2.

Westerhoff, P.; Mezyk, S. P.; Cooper, W. J.; Minakata, D. Electron pulse radiolysis determination of hydroxyl radical rate constants with Suwannee River fulvic acid and other dissolved organic matter isolates *Environ. Sci. Technol.* **2007**, 41 (13) 4640– 4646 DOI: 10.1021/es062529n

[ACS Full Text], [CAS]

3. 3.

Burns, J. M.; Cooper, W. J.; Ferry, J. L.; King, D. W.; DiMento, B. P.; McNeill, K.; Miller, C. J.; Miller, W. L.;Peake, B. M.; Rusak, S. A.; Rose, A. L.; Waite, T. D. Methods for reactive oxygen species (ROS) detection in aqueous environments *Aquat. Sci.* **2012**, 74 (4) 683– 734 DOI: 10.1007/s00027-012-0251-x

[Crossref], [CAS]

4. 4.

Diaz, J. M.; Hansel, C. M.; Voelker, B. M.; Mendes, C. M.; Andeer, P. F.; Zhang, T. Widespread production of extracellular superoxide by heterotrophic bacteria *Science* **2013**, 340 (6137) 1223– 1226 DOI: 10.1126/science.1237331

[Crossref], [PubMed], [CAS]

5. 5.

Nico, P. S.; Anastasio, C.; Zasoski, R. J. Rapid photo-oxidation of Mn(II) mediated by humic substances*Geochim. Cosmochim. Acta* **2002**, 66 (23) 4047– 4056 DOI: 10.1016/S0016-7037(02)01001-3

[Crossref], [CAS]

6. 6.

Learman, D. R.; Voelker, B. M.; Madden, A. S.; Hansel, C. M. Constraints on superoxide mediated formation of manganese oxides *Front. Microbiol.* **2013**, 4, 262 DOI: 10.3389/fmicb.2013.00262

[Crossref], [PubMed], [CAS]

7. 7.

Saragosti, E.; Tchernov, D.; Katsir, A.; Shaked, Y. Extracellular production and degradation of superoxide in the coral *Stylophora pistillata* and cultured *PLoS One* **2010**, 5 (9) e12508 DOI: 10.1371/journal.pone.0012508

[Crossref], [PubMed]

8. 8.

Dorantes-Aranda, J. J.; Seger, A.; Mardones, J. I.; Nichols, P. D.; Hallegraeff, G. M. Progress in understanding algal bloom-eediated fish kills: The role of superoxide radicals, phycotoxins and fatty acids*PLoS One* **2015**, 10 (7) e0133549 DOI: 10.1371/journal.pone.0133549

[Crossref], [PubMed]

9. 9.

Morris, J. J.; Kirkegaard, R.; Szul, M. J.; Johnson, Z. I.; Zinser, E. R. Facilitation of robust growth of prochlorococcus colonies and dilute liquid cultures by “helper” heterotrophic bacteria *Appl. Environ. Microbiol.* **2008**, 74 (14) 4530– 4534 DOI: 10.1128/AEM.02479-07

[Crossref], [PubMed], [CAS]

10. 10.

Tong, M.; Yuan, S.; Ma, S.; Jin, M.; Liu, D.; Cheng, D.; Liu, X.; Gan, Y.; Wang, Y. Production of abundant hydroxyl radicals from oxygenation of subsurface sediments *Environ. Sci. Technol.* **2016**, 50 (1) 214– 221DOI: 10.1021/acs.est.5b04323

[ACS Full Text], [CAS]

11. 11.

Page, S. E.; Kling, G. W.; Sander, M.; Harrold, K. H.; Logan, J. R.; McNeill, K.; Cory, R. M. Dark formation of hydroxyl radical in arctic soil and surface waters *Environ. Sci. Technol.* **2013**, 47 (22) 12860– 12867 DOI: 10.1021/es4033265

[ACS Full Text], [CAS]

12. 12.

Shaked, Y.; Rose, A. Seas of superoxide *Science* **2013**, 340 (6137) 1176– 1177 DOI: 10.1126/science.1240195

[Crossref], [PubMed], [CAS]

13. 13.

Wu, M.; Wong, G. T. F.; Wu, Y.-c.; Shiah, F.-K.; Dai, M. Hydrogen peroxide in tropical shelf waters: The Northern South China Sea Shelf *Deep Sea Res., Part II* **2015**, 117 (0) 143– 154 DOI: 10.1016/j.dsr2.2015.02.027

[Crossref], [CAS]

14. 14.

Yuan, X.; Davis, J. A.; Nico, P. S. Iron-mediated oxidation of methoxyhydroquinone under dark conditions: Kinetic and mechanistic insights *Environ. Sci. Technol.* **2016**, 50 (4) 1731– 1740 DOI: 10.1021/acs.est.5b03939

[ACS Full Text], [CAS]

15. 15.

Pham, A. N.; Waite, T. D. Oxygenation of Fe(II) in natural waters revisited: Kinetic modeling approaches, rate constant estimation and the importance of various reaction pathways *Geochim. Cosmochim. Acta* **2008**,72 (15) 3616– 3630 DOI: 10.1016/j.gca.2008.05.032

[Crossref], [CAS]

16. 16.

Murphy, S. A.; Solomon, B. M.; Meng, S.; Copeland, J. M.; Shaw, T. J.; Ferry, J. L. Geochemical production of reactive oxygen species from biogeochemically reduced Fe *Environ. Sci. Technol.* **2014**, 48 (7) 3815–3821 DOI: 10.1021/es4051764

[ACS Full Text], [CAS]

17. 17.

Pham, A. N.; Xing, G.; Miller, C. J.; Waite, T. D. Fenton-like copper redox chemistry revisited: Hydrogen peroxide and superoxide mediation of copper-catalyzed oxidant production *J. Catal.* **2013**, 301, 54– 64 DOI: 10.1016/j.jcat.2013.01.025

[Crossref], [CAS]

18. 18.

Yuan, X.; Pham, A. N.; Miller, C. J.; Waite, T. D. Copper-catalyzed hydroquinone oxidation and associated redox cycling of copper under conditions typical of natural saline waters *Environ. Sci. Technol.* **2013**, 47 (15)8355– 8364 DOI: 10.1021/es4014344

[ACS Full Text], [CAS]

19. 19.

Yuan, X.; Miller, C. J.; Pham, A. N.; Waite, T. D. Kinetics and mechanism of auto- and copper-catalyzed oxidation of 1,4-naphthohydroquinone *Free Radical Biol. Med.* **2014**, 71 (0) 291– 302 DOI: 10.1016/j.freeradbiomed.2014.03.021

[Crossref], [PubMed], [CAS]

20. 20.

Liu, L.; Yuan, Y.; Li, F.-b.; Feng, C.-h. In-situ Cr(VI) reduction with electrogenerated hydrogen peroxide driven by iron-reducing bacteria *Bioresour. Technol.* **2011**, 102 (3) 2468– 2473 DOI: 10.1016/j.biortech.2010.11.013

[Crossref], [PubMed], [CAS]

21. 21.

Kim, K.; Kim, J.; Bokare, A. D.; Choi, W.; Yoon, H.-I.; Kim, J. Enhanced removal of hexavalent chromium in the presence of H_2O_2 in frozen aqueous solutions *Environ. Sci. Technol.* **2015**, 49 (18) 10937– 10944 DOI: 10.1021/acs.est.5b02702

[ACS Full Text], [CAS]

22. 22.

Pettine, M.; Campanella, L.; Millero, F. J. Arsenite oxidation by H_2O_2 in aqueous solutions *Geochim. Cosmochim. Acta* **1999**, 63 (18) 2727– 2735 DOI: 10.1016/S0016-7037(99)00212-4

[Crossref], [CAS]

23. 23.

Zhang, P.; Yuan, S.; Liao, P. Mechanisms of hydroxyl radical production from abiotic oxidation of pyrite under acidic conditions *Geochim. Cosmochim. Acta* **2016**, 172, 444– 457 DOI: 10.1016/j.gca.2015.10.015

[Crossref], [CAS]

24. 24.

Shaked, Y.; Harris, R.; Klein-Kedem, N. Hydrogen peroxide photocycling in the Gulf of Aqaba, Red Sea*Environ. Sci. Technol.* **2010**, 44 (9) 3238– 3244 DOI: 10.1021/es902343y

[ACS Full Text], [CAS]

25. 25.

Clark, C. D.; De Bruyn, W. J.; Hirsch, C. M.; Aiona, P. Diel cycles of hydrogen peroxide in marine bathing waters in Southern California, USA: In situ surf zone measurements *Mar. Pollut. Bull.* **2010**, 60 (12) 2284–2288 DOI: 10.1016/j.marpolbul.2010.08.004

[Crossref], [PubMed], [CAS]

26. 26.

Steigenberger, S.; Croot, P. L., Identifying the processes controlling the distribution of H_2O_2 in surface waters along a meridional transect in the eastern Atlantic. *Geophys. Res. Lett.* **2008**, 35 (3), DOI: DOI: 10.1029/2007GL032555 .

[Crossref], [PubMed]

27. 27.

Yuan, J.; Shiller, A. M. Distribution of hydrogen peroxide in the northwest Pacific Ocean *Geochem., Geophys., Geosyst.* **2005**, 6 (9) 1– 13 DOI: 10.1029/2004GC000908

[Crossref]

28. 28.

O'Sullivan, D. W.; Neale, P. J.; Coffin, R. B.; Boyd, T. J.; Osburn, C. L. Photochemical production of hydrogen peroxide and methylhydroperoxide in coastal waters *Mar. Chem.* **2005**, 97 (1–2) 14– 33 DOI: 10.1016/j.marchem.2005.04.003

[Crossref], [CAS]

29. 29.

Szymczak, R.; Waite, T. Generation and decay of hydrogen peroxide in estuarine waters *Mar. Freshwater Res.* **1988**, 39 (3) 289– 299 DOI: 10.1071/MF9880289

[Crossref], [CAS]

30. 30.

Febria, C. M.; Lesack, L. F.; Gareis, J. A.; Bothwell, M. L. Patterns of hydrogen peroxide among lakes of the Mackenzie Delta, western Canadian Arctic *Can. J. Fish. Aquat. Sci.* **2006**, 63 (9) 2107– 2118 DOI: 10.1139/f06-106

[Crossref], [CAS]

31. 31.

Wong, A. Y.; Wong, G. T. The effect of spectral composition on the photochemical production of hydrogen peroxide in lake water *Terr Atmos Ocean Sci.* **2001**, 12 (4) 695– 704 DOI: 10.3319/TAO.2001.12.4.695(O)

[Crossref]

32. 32.

Cooper, W. J.; Lean, D. R. S. Hydrogen peroxide concentration in a northern lake: photochemical formation and diel variability *Environ. Sci. Technol.* **1989**, 23 (11) 1425– 1428 DOI: 10.1021/es00069a017

[ACS Full Text], [CAS]

33. 33.

Richard, L. E.; Peake, B. M.; Rusak, S. A.; Cooper, W. J.; Burritt, D. J. Production and decomposition dynamics of hydrogen peroxide in freshwater *Envir. Chem.* **2007**, 4 (1) 49– 54 DOI: 10.1071/EN06068

[Crossref], [CAS]

34. 34.

Rusak, S. A.; Richard, L. E.; Peake, B. M.; Cooper, W. J. Trends in hydrogen peroxide levels in relation to solar radiation in the Water of Leith. Advances in UV studies; Dunedin, New Zealand, **2006**.

35. 35.

Scott, D. T.; Runkel, R. L.; McKnight, D. M.; Voelker, B. M.; Kimball, B. A.; Carraway, E. R. Transport and cycling of iron and hydrogen peroxide in a freshwater stream: Influence of organic acids *Water Resour. Res.***2003**, 39 (11) 1308– 1321 DOI: 10.1029/2002WR001768

[Crossref]

36. 36.

Wilson, C. L.; Hinman, N. W.; Cooper, W. J.; Brown, C. F. Hydrogen peroxide cycling in surface geothermal waters of Yellowstone National Park *Environ. Sci. Technol.* **2000**, 34 (13) 2655– 2662 DOI: 10.1021/es9906397

[ACS Full Text], [CAS]

37. 37.

Wilson, C. L.; Hinman, N. W.; Sheridan, R. P. Hydrogen peroxide formation and decay in iron-rich geothermal waters: the relative roles of abiotic and biotic mechanisms *Photochem. Photobiol.* **2000**, 71 (6)691– 699 DOI: 10.1562/0031-8655(2000)0710691HPFADI2.0.CO2

[Crossref], [PubMed], [CAS]

38. 38.

Yuan, J.; Shiller, A. M. Hydrogen peroxide in deep waters of the North Pacific Ocean. *Geophys. Res. Lett.***2004**, 31 (1), DOI: DOI: 10.1029/2003GL018439 .

[Crossref]

39. 39.

Vermilyea, A. W.; Paul Hansard, S.; Voelker, B. M. Dark production of hydrogen peroxide in the Gulf of Alaska *Limnol. Oceanogr.* **2010**, 55 (2) 580– 588 DOI: 10.4319/lo.2010.55.2.0580

[Crossref], [CAS]

40. 40.

Roe, K. L.; Schneider, R. J.; Hansel, C. M.; Voelker, B. M. Measurement of dark, particle-generated superoxide and hydrogen peroxide production and decay in the subtropical and temperate North Pacific Ocean *Deep Sea Res., Part I* **2016**, 107, 59– 69 DOI: 10.1016/j.dsr.2015.10.012

[Crossref], [CAS]

41. 41.

Lee, M.; Heikes, B. G.; O'Sullivan, D. W. Hydrogen peroxide and organic hydroperoxide in the troposphere: a review *Atmos. Environ.* **2000**, 34 (21) 3475– 3494 DOI: 10.1016/S1352-2310(99)00432-X

[Crossref], [CAS]

42. 42.

Kieber, R. J.; Peake, B.; Willey, J. D.; Jacobs, B. Iron speciation and hydrogen peroxide concentrations in New Zealand rainwater *Atmos. Environ.* **2001**, 35 (34) 6041– 6048 DOI: 10.1016/S1352-2310(01)00199-6

[Crossref], [CAS]

43. 43.

Sakugawa, H.; Kaplan, I. R.; Tsai, W.; Cohen, Y. Atmospheric hydrogen peroxide *Environ. Sci. Technol.***1990**, 24 (10) 1452– 1462 DOI: 10.1021/es00080a002

[ACS Full Text], [CAS]

44. 44.

Mullaugh, K. M.; Kieber, R. J.; Willey, J. D.; Avery, G. B. Long-term temporal variability in hydrogen peroxide concentrations in Wilmington, North Carolina USA rainwater *Environ. Sci. Technol.* **2011**, 45 (22) 9538–9542 DOI: 10.1021/es202634s

[ACS Full Text], [CAS]

45. 45.

He, S.; Chen, Z.; Zhang, X.; Zhao, Y.; Huang, D.; Zhao, J.; Zhu, T.; Hu, M.; Zeng, L. Measurem ent of atmospheric hydrogen peroxide and organic peroxides in Beijing before and during the 2008 Olympic Games: Chemical and physical factors influencing their concentrations. *J. Geophys. Res.* **2010**, 115 (D17), DOI: DOI: 10.1029/2009JD013544 .

[Crossref], [PubMed]

46. 46.

Encrenaz, T.; Greathouse, T. K.; Lefèvre, F.; Atreya, S. K. Hydrogen peroxide on Mars: Observations, interpretation and future plans *Planet. Space Sci.* **2012**, 68 (1) 3– 17 DOI: 10.1016/j.pss.2011.03.019

[Crossref], [CAS]

47. 47.

Encrenaz, T.; Bézard, B.; Greathouse, T. K.; Richter, M. J.; Lacy, J. H.; Atreya, S. K.; Wong, A. S.;Lebonnois, S.; Lefèvre, F.; Forget, F. Hydrogen peroxide on Mars: evidence for spatial and seasonal variations *Icarus* **2004**, 170 (2) 424– 429 DOI: 10.1016/j.icarus.2004.05.008

[Crossref], [CAS]

48. 48.

Yabusaki, S. B.; Fang, Y.; Long, P. E.; Resch, C. T.; Peacock, A. D.; Komlos, J.; Jaffe, P. R.; Morrison, S. J.;Dayvault, R. D.; White, D. C.; Anderson, R. T. Uranium removal from groundwater via in situ biostimulation: Field-scale modeling of transport and biological processes *J. Contam. Hydrol.* **2007**, 93 (1–4) 216– 235 DOI: 10.1016/j.jconhyd.2007.02.005

[Crossref], [PubMed], [CAS]

49. 49.

Janot, N.; Lezama Pacheco, J. S.; Pham, D. Q.; O'Brien, T. M.; Hausladen, D.; Noël, V.; Lallier, F.;Maher, K.; Fendorf, S.; Williams, K. H.; Long, P. E.; Bargar, J. R. Physico-chemical feterogeneity of organic-rich sediments in the Rifle aquifer, CO: Impact on uranium biogeochemistry *Environ. Sci. Technol.* **2016**, 50(1) 46– 53 DOI: 10.1021/acs.est.5b03208

[ACS Full Text], [CAS]

50. 50.

King, D. W.; Cooper, W. J.; Rusak, S. A.; Peake, B. M.; Kiddle, J. J.; O'Sullivan, D. W.; Melamed, M. L.;Morgan, C. R.; Theberge, S. M. Flow injection analysis of H_2O_2 in natural waters using acridinium ester chemiluminescence: Method development and optimization using a kinetic model *Anal. Chem.* **2007**, 79 (11)4169– 4176 DOI: 10.1021/ac062228w

[ACS Full Text], [CAS]

51. 51.

Cooper, W. J.; Moegling, J. K.; Kieber, R. J.; Kiddle, J. J. A chemiluminescence method for the analysis of H_2O_2 in natural waters *Mar. Chem.* **2000**, 70 (1–3) 191– 200 DOI: 10.1016/S0304-4203(00)00025-6

[Crossref], [CAS]

52. 52.

American Society for Testing Materials. Standard test methods for low-level dissolved oxygen in water; ASTM D 5543-5549; ASTM: Philadelphia, **1995**.

53. 53.

Gilbert, T.; Behymer, T.; Castaneda, H. Determination of dissolved-oxygen in natural and wastewaters *Am. Lab.* **1982**, 14 (3) 119– 134

[CAS]

54. 54.

Johnson, K. A.; Simpson, Z. B.; Blom, T. Global Kinetic Explorer: A new computer program for dynamic simulation and fitting of kinetic data *Anal. Biochem.* **2009**, 387 (1) 20– 29 DOI: 10.1016/j.ab.2008.12.024

[Crossref], [PubMed], [CAS]

55. 55.

Yuan, J.; Shiller, A. M. The distribution of hydrogen peroxide in the southern and central Atlantic ocean*Deep Sea Res., Part II* **2001**, 48 (13) 2947– 2970 DOI: 10.1016/S0967-0645(01)00026-1

[Crossref], [CAS]

56. 56.

Zachara, J. M.; Long, P. E.; Bargar, J.; Davis, J. A.; Fox, P.; Fredrickson, J. K.; Freshley, M. D.;Konopka, A. E.; Liu, C.; McKinley, J. P.; Rockhold, M. L.; Williams, K. H.; Yabusaki, S. B. Persistence of uranium groundwater plumes: Contrasting mechanisms at two DOE sites in the groundwater–river interaction zone *J. Contam. Hydrol.* **2013**, 147, 45– 72 DOI: 10.1016/j.jconhyd.2013.02.001

[Crossref], [PubMed], [CAS]

57. 57.

Page, S. E.; Sander, M.; Arnold, W. A.; McNeill, K. Hydroxyl radical formation upon oxidation of reduced humic acids by oxygen in the dark *Environ. Sci. Technol.* **2012**, 46 (3) 1590– 1597 DOI: 10.1021/es203836f

[ACS Full Text], [CAS]

58. 58.

Fox, P. M.; Davis, J. A.; Hay, M. B.; Conrad, M. E.; Campbell, K. M.; Williams, K. H.; Long, P. E. Rate-limited U(VI) desorption during a small-scale tracer test in a heterogeneous uranium-contaminated aquifer *Water Resour. Res.* **2012**, 48 (5) W05512 DOI: 10.1029/2011WR011472

[Crossref], [CAS]

59. 59.

Yamasaki, Y.; Kim, D.-I.; Matsuyama, Y.; Oda, T.; Honjo, T. Production of superoxide anion and hydrogen peroxide by the red tide dinoflagellate Karenia mikimotoi *J. Biosci. Bioeng.* **2004**, 97 (3) 212– 215 DOI: 10.1016/S1389-1723(04)70193-0

[Crossref], [PubMed], [CAS]

60. 60.

Rose, A. L.; Godrant, A.; Furnas, M.; Waite, T. D. Dynamics of nonphotochemical superoxide production in the Great Barrier Reef lagoon *Limnol. Oceanogr.* **2010**, 55 (4) 1521– 1536 DOI: 10.4319/lo.2010.55.4.1521

[Crossref], [CAS]

61. 61.

Duesterberg, C. K.; Waite, T. D. Process optimization of Fenton oxidation using kinetic modeling *Environ. Sci. Technol.* **2006**, 40 (13) 4189– 4195 DOI: 10.1021/es060311v

[ACS Full Text], [CAS]

62. 62.

Keenan, C. R.; Sedlak, D. L. Ligand-enhanced reactive oxidant generation by nanoparticulate zero-valent iron and oxygen *Environ. Sci. Technol.* **2008**, 42 (18) 6936– 6941 DOI: 10.1021/es801438f

[ACS Full Text], [CAS]

63. 63.

Jiang, C.; Garg, S.; Waite, T. D. Hydroquinone-mediated redox cycling of iron and concomitant oxidation of hydroquinone in oxic waters under acidic conditions: Comparison with iron-natural organic matter interactions *Environ. Sci. Technol.* **2015**, 49 (24) 14076– 14084 DOI: 10.1021/acs.est.5b03189

[ACS Full Text], [CAS]

64. 64.

Borda, M. J.; Elsetinow, A. R.; Strongin, D. R.; Schoonen, M. A. A mechanism for the production of hydroxyl radical at surface defect sites on pyrite *Geochim. Cosmochim. Acta* **2003**, 67 (5) 935– 939 DOI: 10.1016/S0016-7037(02)01222-X

[Crossref], [CAS]

65. 65.

Minella, M.; De Laurentiis, E.; Maurino, V.; Minero, C.; Vione, D. Dark production of hydroxyl radicals by aeration of anoxic lake water *Sci. Total Environ.* **2015**, 527–528, 322– 327 DOI: 10.1016/j.scitotenv.2015.04.123

[Crossref], [PubMed], [CAS]

66. 66.

Petasne, R. G.; Zika, R. G. Fate of superoxide in coastal sea water *Nature* **1987**, 325 (6104) 516– 518 DOI: 10.1038/325516a0

[Crossref], [CAS]

67. 67.

Cooper, W. J.; Zika, R. G.; Petasne, R. G.; Plane, J. M. C. Photochemical formation of hydrogen peroxide in natural waters exposed to sunlight *Environ. Sci. Technol.* **1988**, 22 (10) 1156– 1160 DOI: 10.1021/es00175a004

[ACS Full Text], [CAS]

68. 68.

Chin, Y.-P.; Miller, P. L.; Zeng, L.; Cawley, K.; Weavers, L. K. Photosensitized degradation of bisphenol A by dissolved organic matter *Environ. Sci. Technol.* **2004**, 38 (22) 5888– 5894 DOI: 10.1021/es0496569

[ACS Full Text], [CAS]

69. 69.

Davis, J. A.; Smith, R.; Bohlke, J. K.; Jemison, N.; Huang, X.; Repert, D.; Yuan, X.; Williams, K. H. Oxidation of naturally reduced uranium in aquifer sediments by dissolved oxygen and its potential significance to uranium plume persistence. In preparation.

70. 70.

Kuzyakov, Y.; Blagodatskaya, E. Microbial hotspots and hot moments in soil: Concept & review *Soil Biol. Biochem.* **2015**, 83, 184– 199 DOI: 10.1016/j.soilbio.2015.01.025

[Crossref], [CAS]

71. 71.

Rose, A. L.; Webb, E. A.; Waite, T. D.; Moffett, J. W. Measurement and implications of nonphotochemically generated superoxide in the Equatorial Pacific Ocean *Environ. Sci. Technol.* **2008**, 42 (7) 2387– 2393 DOI: 10.1021/es7024609

[ACS Full Text], [CAS]

72. 72.

Dixon, T. C.; Vermilyea, A. W.; Scott, D. T.; Voelker, B. M. Hydrogen peroxide dynamics in an agricultural headwater stream: Evidence for significant nonphotochemical production *Limnol. Oceanogr.* **2013**, 58 (6)2133– 2144 DOI: 10.4319/lo.2013.58.6.2133

[Crossref], [CAS]

73. 73.

Garg, S.; Ito, H.; Rose, A. L.; Waite, T. D. Mechanism and kinetics of dark iron redox transformations in previously photolyzed acidic natural organic matter solutions *Environ. Sci. Technol.* **2013**, 47 (4) 1861– 1869DOI: 10.1021/es3035889

[ACS Full Text], [CAS]

74. 74.

Weiss, J. Electron transition process in the mechanism of oxidation and reduction reactions in solutions*Naturwissenschaften* **1935**, 23, 64– 69 DOI: 10.1007/BF01497021

[Crossref], [CAS]

75. 75.

King, D. W.; Lounsbury, H. A.; Millero, F. J. Rates and mechanism of Fe(II) oxidation at nanomolar total iron concentrations *Environ. Sci. Technol.* **1995**, 29 (3) 818– 824 DOI: 10.1021/es00003a033

[ACS Full Text], [CAS]

76. 76.

Rose, A. L.; Waite, T. D. Chemiluminescence of luminol in the presence of iron(II) and oxygen: Oxidation mechanism and implications for its analytical use *Anal. Chem.* **2001**, 73 (24) 5909– 5920 DOI: 10.1021/ac015547q

[ACS Full Text], [CAS]

77. 77.

Jones, A. M.; Griffin, P. J.; Collins, R. N.; Waite, T. D. Ferrous iron oxidation under acidic conditions – The effect of ferric oxide surfaces *Geochim. Cosmochim. Acta* **2014**, 145, 1– 12 DOI: 10.1016/j.gca.2014.09.020

[Crossref], [CAS]

78. 78.

Schoonen, M. A. A.; Harrington, A. D.; Laffers, R.; Strongin, D. R. Role of hydrogen peroxide and hydroxyl radical in pyrite oxidation by molecular oxygen *Geochim. Cosmochim. Acta* **2010**, 74 (17) 4971– 4987 DOI: 10.1016/j.gca.2010.05.028

[Crossref], [CAS]

79. 79.

Miller, C. J.; Waite, T. D. Transient oxidant production during the oxidation of iron(II) monosulfides at pH 8. Goldschmidt Abstracts, June 26–July 1, **2016**; 2847.

80. 80.

Cheng, D.; Yuan, S.; Liao, P.; Zhang, P. Oxidizing impact induced by mackinawite (fes) nanoparticles at oxic conditions due to production of hydroxyl radicals *Environ. Sci. Technol.* **2016**, 50 (21) 11646– 11653 DOI: 10.1021/acs.est.6b02833

[ACS Full Text], [CAS]

81. 81.

Southworth, B. A.; Voelker, B. M. Hydroxyl radical production via the photo-Fenton reaction in the presence of fulvic acid *Environ. Sci. Technol.* **2003**, 37 (6) 1130– 1136 DOI: 10.1021/es020757l

[ACS Full Text], [CAS]

82. 82.

Herut, B.; Shoham-Frider, E.; Kress, N.; Fiedler, U.; Angel, D. L. Hydrogen peroxide production rates in clean and polluted coastal marine waters of the Mediterranean, Red and Baltic Seas *Mar. Pollut. Bull.* **1998**,36 (12) 994– 1003 DOI: 10.1016/S0025-326X(98)80004-0

[Crossref], [CAS]

83. 83.

Schmidt, M. W.; Torn, M. S.; Abiven, S.; Dittmar, T.; Guggenberger, G.; Janssens, I. A.; Kleber, M.;Kögel-Knabner, I.; Lehmann, J.; Manning, D. A.Persistence of soil organic matter as an ecosystem property *Nature* **2011**, 478 (7367) 49– 56 DOI: 10.1038/nature10386

[Crossref], [PubMed], [CAS]